2021 43rd Annual International Conference of the
IEEE Engineering in Medicine & Biology Society (EMBC)
Oct 31 - Nov 4, 2021. Virtual Conference

2021 43rd Annual International Conference of the IEEE Engineering in Medicine & Biology Society (EMBC) | 978-1-7281-1179-7/21/$31.00 ©2021 IEEE | DOI: 10.1109/EMBC46164.2021.9630998

Comparing Machine Learning Methods and Feature Extraction Techniques for the EMG Based Decoding of Human Intention

Amber Turner*, Dasha Shieff*, Anany Dwivedi, and Minas Liarokapis

Abstract— **With an increasing number of robotic and prosthetic devices, there is a need for intuitive Muscle-Machine Interfaces (MuMIs) that allow the user to have an embodied interaction with the devices they are controlling. Such MuMIs can be developed using machine learning based methods that utilize myoelectric activations from the muscles of the user to decode their intention. However, the choice of the learning method is subjective and depends on the features extracted from the raw Electromyography signals as well as on the intended application. In this work, we compare the performance of five machine learning methods and eight time-domain feature extraction techniques in discriminating between different gestures executed by the user of an EMG based MuMI. From the results, it can be seen that the Willison Amplitude performs consistently better for all the machine learning methods compared in this study, while the Zero Crossings achieves the worst results for the Decision Trees and the Random Forests and the Variance offers the worst performance for all the other learning methods. The Random Forests method is shown to achieve the best results in terms of achieved accuracies (has the lowest variance between subjects). In order to experimentally validate the efficiency of the Random Forest classifier and the Willison Amplitude technique, a series of gestures were decoded in a real-time manner from the myoelectric activations of the operator and they were used to control a robot hand.**

I. Introduction

Over the last decades, an increased number of robotic and mechatronic devices have been introduced in our day-to-day life and new means of interacting with them have been tested. In particular, nowadays there is a need for intuitive methods of interfacing with such devices as the traditional interfaces (e.g. buttons, hand-held controllers, vision and voice based interaction systems) are often inconvenient, awkward in social situations, and difficult to use [1]. To alleviate the above mentioned issues, Muscle Machine Interfaces (MuMIs) can be employed. These interfaces utilize myoelectric activations to decode human intentions providing an immersive interaction with various devices. Another advantage of such electromyography (EMG) based interfaces is that they can be hands-free, which allows the user to have a more natural interaction with devices in different applications (e.g. teleoperation of robot arms [2], control of prostheses).

The development of a mathematical model of the human musculoskeletal system has been of great interest to bioengineers and neurophysiologists. In 1938 a model was proposed by Hill [3], which is known as the Hill-Type muscle model.

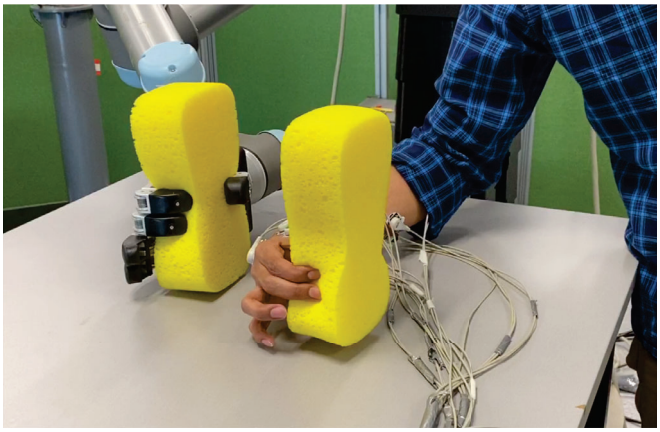

Fig. 1. Real-time control of the New Dexterity five fingered robotic hand using a muscle-machine interface that discriminates between appropriate grasping postures, gestures, and actions.

This model employs several internal parameters, like, muscle fiber length and muscle contraction velocity, which vary from person to person. Due to these parameters, it requires a complex calibration procedure to develop subject and muscle specific models. To overcome this issue, researchers have focused on machine learning based approaches [4].

Machine learning based MuMI intefaces can be categorized as: i) classification based interfaces [5], [6] and ii) regression based interfaces [7], [8]. The output of classification based methods is a discrete decision on the intention of the user (i.e., identifying the task to be executed), while regression methods provide a continuous prediction of the human intention (i.e., deriving specific motion trajectories). The processing pipeline for developing EMG based interfaces using machine learning based methods consists of data acquisition, signal filtering, feature extraction, and classification of the patterns of the various gestures [9]. To remove the inherent signal noise as well as the electromagnetic interference, the acquired EMG signal is filtered [10]. It should also be noted that the required processing should be completed in a time efficient manner, to classify the acquired signals while meeting the real-time requirement of practical applications.

The raw EMG data needs to be appropriately pre-processed before extracting the features. The first step in pre-processing involves filtering to remove unwanted noise in the signal. In [11], the authors reduce the motion artifacts in the signal using a bandpass filter (20 Hz - 500 Hz). After filtering the acquired signals, the data is then segmented to compute the feature set to be extracted from the raw

*These authors contributed equally to this work.

Amber Turner, Dasha Shieff, Anany Dwivedi, and Minas Liarokapis are with the New Dexterity research group, Department of Mechanical Engineering, The University of Auckland, New Zealand. E-mails: {atur439, dshi310, adwi592}@aucklanduni.ac.nz, minas.liarokapis@auckland.ac.nz

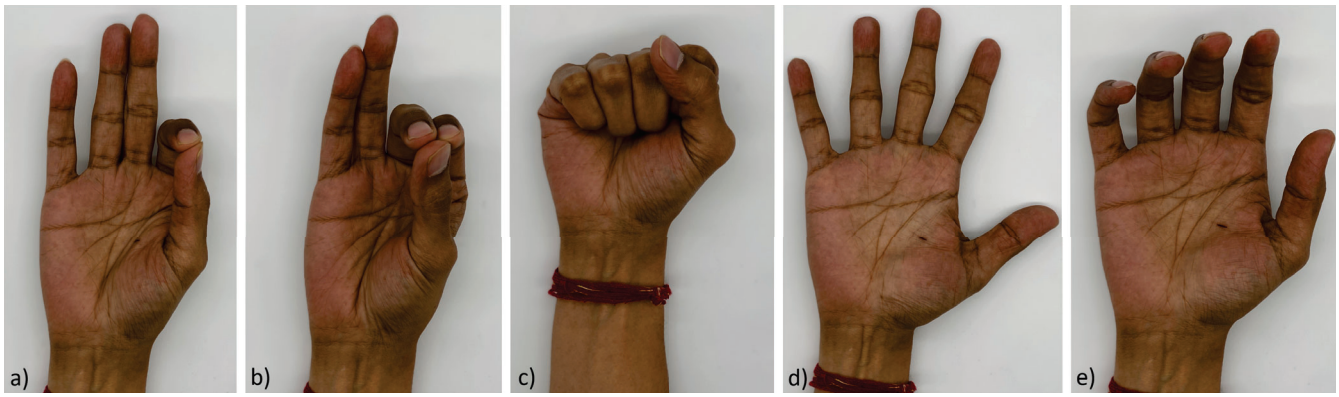

Fig. 2. The grasping postures, gestures, and actions examined in this study. Subfigure a) shows the pinch grasp, subfigure b) shows the tripod grasp, subfigure c) shows the power grasp, subfigure d) shows an open hand configuration with abducted fingers, and subfigure e) shows the rest state. The final action executed in this study is co-contraction of all muscles, which is not shown as it can be achieved with many different gestures or postures.

EMG data. The segment length for calculating the features is important as it affects the performance of machine learning based intention decoding models [12]. According to previous studies, a segment length smaller than 125 ms results in high bias and variance in the calculated features, while a segment length between 125 ms and 500 ms increases the classification accuracy significantly by reducing the bias and variance in the calculated features [13], [14]. However, for real-time control of devices (e.g. control of prosthetic limbs or robotic end-effectors), the response time of the interface is required to be less than 300 ms [15].

Meaningful information can be extracted from the raw EMG signals using feature extraction methods. These methods can be classified into three different categories, Time Domain (TD) features, Frequency Domain (FD) features or Time-Frequency Domain (TFD) features [16]. The TD features are used to extract the information from the amplitude of the EMG signals, FD features provide the information regarding the Power Spectral Density (PSD), while TFD features are a combination of amplitudes and the PSD of the signal. According to past studies [17], [18], TD features provide a more consistent performance over time than FD.

In [19], authors employed four TD features, namely, Mean Absolute Value (MAV), Slope Sign Changes (SSC), Zero Crossing (ZC), and Waveform Length (WL) for control of a prosthesis using EMG signals. In [18], authors show that RMS performs better as compared to MAV, maximum amplitude (MAX), SSC, ZC, and WL as it provides a quantitative measure for electrode selection. In [20], Anam et al. classified individual finger movements using myoelectric activations of the muscles of the forearm and TD features. To achieve this, they employed Spectral Regression Discriminant Analysis (a modified version of Linear Discriminant Analysis) to reduce the dimensionality of the problem and an Extreme Learning Machine to classify the finger movements.

After feature extraction, classification methods are used to map processed EMG data associated with a specific gesture to a control output. Random Forest (RF), K-Nearest Neighbors (KNN), Support Vector Machines (SVMs), Linear Discriminant Analysis (LDA), and Neural Network (NN)

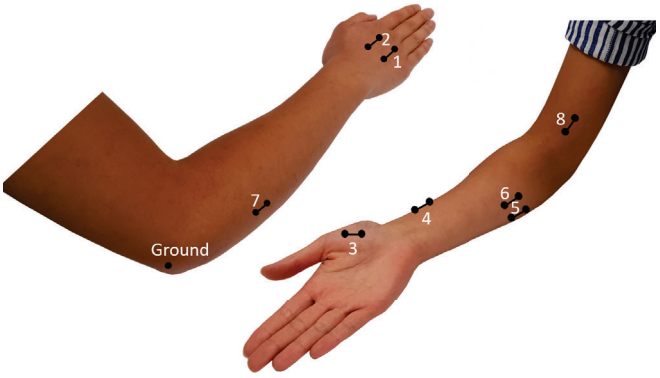

Fig. 3. Placement of electrodes on the right human arm for EMG data collection. The double dot with the connected line represents a double differential EMG electrode. Ground is represented with a single dot and is placed on the elbow where muscular activity is minimal.

are among the methods that have been implemented by various authors [21]–[25] resulting in different success rates and classification accuracies ranging between $70-90\%$. The choice of learning method is subjective and depends on the features extracted from the raw Electromyography signals as well as on the intended application. Several factors that affect this decision are the accuracy, type of input data needed, and computational complexity of the different methods.

In this work, we compare the performance of five machine learning methods and eight time-domain feature extraction techniques in discriminating between different gestures executed by the user of an EMG based MuMI. The goal of this study is to inform other researchers about the most promising combinations of extracted features and machine learning methods that offer excellent performance. To do this, eight different TD features are extracted, while five different classification based machine learning methods are employed to develop gesture decoding models. Finally, an RF methodology based decoding framework is implemented so as to control the New Dexterity five fingered, anthropomorphic robot hand [26] in the execution of various postures and gestures (as seen in Fig. 1).

The rest of the paper is organized as follows: Section II describes the apparatus used and the experimental setup. The extracted features and the machine learning methods employed are discussed in section III. Finally, section IV presents the results, while section V concludes the work.

II. Apparatus and Experiments

The study has received the approval of the University of Auckland Human Participants Ethics Committee (UAHPEC) with the reference number #019043. Prior to the study all participants provided written and informed consent to the experimental procedures. The experiments were performed by 6 able-bodied subjects (age = 24 ± 3), four males and two females. The experiments were performed by subjects with their dominant hand. Four subjects (two males and two females) were right hand dominant and two subjects (both males) were left hand dominant.

A. Experimental Setup

The myoelectric activations for decoding the user intention were captured using a g.Tec g.USBamp bioamplifier. The sampling rate used for the data acquisition was 1200 Hz and the acquired signal was bandpass filtered using a Butterworth filter (5 Hz-500 Hz). A notch filter of 50 Hz was applied to reduce the electric noise. For the experiments, each subject was instructed to alternate between a rest state and a gesture state. In total six gestures were recorded: i) a pinch grasp, ii) a tripod grasp, iii) a power grasp, iv) an open hand configuration with abducted fingers, v) co-contraction of all muscles, and vi) rest state (see Fig. 2). The data acquisition framework was implemented within the Robot Operating System (ROS) [27], which offers the necessary communication, testing, and visualization utilities. The subjects were presented a visual cue at the beginning and termination of each grasp in sequence on the computer screen in the form of a three second countdown timer. To facilitate the labeling of the acquired data for developing supervised learning models, a software trigger was sent to the data recording script to isolate the rest phase from the gesture phase, when the visual cues were presented to the subject. For each gesture, ten seconds of rest state were recorded followed by ten seconds of gesture execution with five repetitions each.

B. Muscle Selection

The myoelectric activations of eight muscle groups of the hand and forearm were recorded using a bipolar electrode setup. The first channel was placed at the back of the hand focusing on the third dorsoral interossei while the second channel was placed on the second dorsoral interossei to distinguish between pinch and tripod gestures. The third channel was placed on the opponens pollicis and the forth channel was placed on abductor pollicis longus to capture the activity of the thumb. Channels 5 and 6 were placed on the flexor digitorum muscle site. Channel 7 was placed on the extensor digitorum muscle site and channel 8 was placed on the bicep brachii muscle site. The ground electrode was placed on the elbow bone, where the myoelectric activity is minimal. Fig. 3 shows the electrode placement on the right human arm-hand system.

III. Methods

This section describes the TD features extracted from the raw EMG data, along with the different machine learning methods used to develop intention decoding models.

A. Feature Extraction

In this study, raw EMG signals were acquired and filtered (5 Hz - 500 Hz Butterworth filter) by the bioamplifier. These signals were then segmented for feature extraction using a sliding window of 166.67 ms with increments of 16.67 ms. The size and the stride (increment interval) of the window size were selected to optimize performance. The performance of the decoding models depend on the window size and the stride. The size of the window must not be too large due to the real-time requirement of practical applications. But, the window should be adequately large to avoid high biases and variance [28]. In this work, the eight different TD features were extracted from each EMG channel to develop machine learning based models for decoding different hand gestures. The features examined are as follows: Root Mean Square Value (RMS), Waveform Length (WL), Zero Crossings (ZC), Integrated EMG (IEMG), Mean Absolute Value (MAV), Willison Amplitude (WAMP), Variance (VAR), and Log Detector (LogD) [29]–[33]. More precisely, we provide detailed descriptions:

1) Root Mean Square: The RMS of the EMG signal is one of the most commonly used values in the TD. It represents the square root of the average power of the signal for the given time period.

2) Waveform Length: WL measures the complexity of the signal. It represents the amplitude of the waveform, frequency, and duration in a single parameter.

3) Zero Crossings: ZC provides rough FD information and represents the number of times the signal crosses the zero value in a given time period. ZC can also be used to estimate the fatigue in the muscles.

4) Integrated EMG: IEMG is the summation of the absolute values of the EMG signal amplitude. It is generally used as an onset index to detect the muscle activity.

5) Mean Absolute Value: MAV can be calculated by taking the average of the absolute value of the EMG signal. It is similar to IEMG which detects the onset of muscle activity. It also provides information regarding the muscle contraction levels.

6) Willison Amplitude: WAMP represents the number of times that the difference between EMG signal amplitude among two consecutive values exceed a predefined threshold. WAMP is related to the firing of motor unit action potentials (MUAP) and the muscle contraction level.

7) Variance: VAR of the myoelectric activations measures the power of the signal. Variance is the mean value of the square of the deviation of that variable.

TABLE I

SUMMARY OF THE FEATURES COMPARED WITH CORRESPONDING FORMULAE AND DESCRIPTIONS.

Feature Extraction Methods	**Formula**	**Description**
Root Mean Square (RMS)	$RMS = \sqrt{\frac{1}{N}\sum_{i=1}^{N} x_i^2}$	Represents the average power of the signal.
Waveform Length (WL)	$WL = \sum_{i=1}^{N-1} \lvert x_{i+1} - x_i \rvert$	Measure of complexity of the EMG signal.
Zero Crossings (ZC)	$x_k < 0 \quad \&\& \quad x_{k+1} > 0$ $\lVert\lVert$ $x_k > 0 \quad \&\& \quad x_{k+1} < 0$ $\&\&$ $\lvert x_k - x_{k+1} \rvert > V_t$	Indicator of fatigue in muscles.
Integrated EMG (IEMG)	$IEMG = \sum_{i=1}^{N} \lvert x_i \rvert$	Detects the onset of muscle activity.
Mean Absolute Value (MAV)	$MAV = \frac{1}{N}\sum_{i=1}^{N} \lvert x_i \rvert$	Measures the contraction level of muscles.
Willison Amplitude (WAMP)	$WAMP = \sum_{i=1}^{N-1}[f(\lvert x_n - x_{n+1} \rvert)]$ $\begin{cases} 1 & x \geq threshold \\ 0 & otherwise \end{cases}$	Measures the contraction level of muscles.
Variance (VAR)	$VAR = \frac{1}{N-1}\sum_{i=1}^{N} x_i^2$	Measure of EMG signal power.
Log Detector (LogD)	$LOG = e^{\frac{1}{N}\sum_{i=1}^{N} log(\lvert x_i \rvert)}$	Provides an estimate of the muscle contraction force.

8) Log Detector: LogD also provides an estimate of the muscle contraction force.

A summary of all the different features that were calculated and examined in this study along with details regarding the calculation of each feature can be found in Table I.

B. Machine Learning Methods

In this work, we chose to train a series of gesture decoding models using five different machine learning methods, namely: Decision Trees (DT), Random Forests (RF), Linear Discriminant Analysis (LDA), Support Vector Machines (SVM), and Neural Networks (NN) [34]–[36]. For each learning method examined, eight different decoding models were developed using each one of the extracted features at a time. The ability of the models to discriminate between the different grasping postures and gestures was evaluated employing the 5-fold cross-validation method.

IV. RESULTS

In this section, we present the gesture decoding performance of each of the machine learning methods analyzed in this study. To do this, we train different gesture decoding models using each extracted EMG feature. In order to avoid any biases in the accuracy values as a result of an imbalanced dataset, it was ensured that the training set and the validation set are balanced, i.e., the number of data points for each grasp type were made to be equal in both the sets. The presented results are the average values calculated using the 5-fold cross-validation procedure.

Table II shows the accuracy of the trained models in decoding the selected gestures. The best and the worst performing features are highlighted for each decoding model (which are trained for each subject using only one feature at a time). It can be noticed that the learning models developed using only the WAMP feature perform consistently better as compared to the decoding models developed using the other features. MAV and IEMG have identical performances for all the machine learning methods except for SVMs for which MAV performs significantly better than IEMG. It can also be noticed from Table II, that for DT and RF based models ZC is the worst performing feature, while for LDA, SVM, and NN, VAR has the worst performance.

As a result of a consistent performance, RF based models were selected to demonstrate their real-time gesture decoding capabilities using the WAMP feature. The decoded gestures were mapped to the NDX-A* five-fingered anthropomorphic robot hand [26]. The demonstrations for the real-time gesture execution on the robot hand were recorded and the compiled video is available in HD quality at the following URL:

www.newdexterity.org/FeatureExtraction

TABLE II

GESTURE CLASSIFICATION ACCURACY FOR DIFFERENT MACHINE LEARNING MODELS TRAINED USING EACH EXTRACTED FEATURE. THE BEST AND WORST PERFORMING FEATURES ARE HIGHLIGHTED FOR EACH SUBJECT. HIGHEST ACCURACY FOR EACH SUBJECT IS UNDERLINED AND HIGHLIGHTED IN BLUE WHILE THE LOWEST ACCURACY IS HIGHLIGHTED IN YELLOW.

Machine Learning Method	Subjects	RMS	WL	ZC	MAV	IEMG	WAMP	VAR	LogD
Decision Tree	1	95.18	94.14	83.15	95.26	95.26	96.21	95.18	95.22
	2	86.46	87.43	86.08	83.25	83.25	84.12	86.47	84.61
	3	84.32	84.49	71.33	82.66	82.66	85.06	84.34	81.57
	4	88.41	92.55	71.34	90.50	90.50	91.43	88.42	89.33
	5	92.74	92.58	90.61	93.20	93.20	95.79	92.75	93.06
	6	92.87	91.36	83.34	94.09	94.09	91.71	92.87	92.65
Random Forest	1	94.76	95.12	84.95	95.05	95.21	96.55	94.81	95.62
	2	90.15	85.92	84.16	90.35	90.54	83.79	91.62	90.28
	3	83.83	86.17	73.90	84.06	84.34	85.09	83.79	82.97
	4	90.86	93.36	72.82	90.44	90.24	92.52	90.33	89.32
	5	93.82	94.48	91.23	93.62	93.69	96.40	94.71	93.62
	6	93.12	87.99	86.12	91.09	95.17	90.63	94.68	87.86
Linear Discriminant Analysis	1	94.89	94.42	80.62	94.70	94.70	95.84	78.26	94.16
	2	91.39	91.19	87.20	90.87	90.87	87.63	82.95	89.89
	3	71.78	88.61	75.05	71.11	71.11	92.47	51.58	67.52
	4	80.14	82.30	69.14	79.76	79.76	85.70	63.48	77.77
	5	92.62	91.54	88.29	92.58	92.58	97.43	58.99	91.87
	6	92.70	92.23	80.82	92.43	92.43	96.31	72.47	91.44
Support Vector Machine	1	96.25	73.04	82.42	94.86	50.41	94.17	52.91	96.07
	2	89.49	50.27	87.49	89.65	34.30	88.62	19.57	92.01
	3	83.69	61.48	75.88	84.77	35.71	93.62	25.50	83.01
	4	91.18	61.36	70.86	91.39	46.47	91.06	28.24	91.88
	5	95.18	71.19	88.31	95.62	49.21	96.46	51.63	95.46
	6	94.53	70.59	83.03	89.87	43.36	93.02	32.30	89.52
Neural Network	1	81.00	79.98	69.38	80.78	80.76	80.69	69.14	80.04
	2	77.39	77.58	72.92	74.68	77.03	71.58	61.78	78.25
	3	45.21	71.36	69.51	39.51	41.95	80.98	20.76	35.60
	4	60.16	63.01	61.96	56.72	59.97	72.51	32.55	54.76
	5	72.66	80.33	74.55	80.32	74.40	82.34	40.66	69.27
	6	79.99	81.83	72.97	79.08	79.74	79.81	47.46	76.24

V. CONCLUSION

In this work, we compared the performance of five machine learning methods and eight time-domain feature extraction techniques in discriminating between different grasping postures and gestures executed by the user of an EMG based Muscle Machine Interface. The postures and gestures considered were: a pinch grasp, a tripod grasp, a power grasp, an open hand configuration with the fingers abducted, a muscle co-contraction state, and the rest state. From the results, it can be seen that Willison Amplitude performs provides the best results for all machine learning methods compared in this study. It can also be seen that the Zero Crossings achieves the worst results for the Decision Trees and the Random Forests and the Variance offers the worst performance for all the other learning methods. Finally, to experimentally validate the efficiency of the Random Forest classifier and the Willison Amplitude feature extraction technique, a series of gestures were decoded in real-time from the myoelectric activations of a user and they were used to control the New Dexterity NDX-A* humanlike robot hand.

REFERENCES

[1] A. Dwivedi, Y. Kwon, and M. Liarokapis, "EMG-Based Decoding of Manipulation Motions in Virtual Reality: Towards Immersive Interfaces," in *International Conference on Systems, Man, and Cybernetics (SMC)*. IEEE, 2020, pp. 3296–3303.

[2] P. K. Artemiadis and K. J. Kyriakopoulos, "Emg-based position and force control of a robot arm: Application to teleoperation and orthosis," in *2007 IEEE/ASME international Conference on advanced intelligent mechatronics*. IEEE, 2007, pp. 1–6.

[3] A. V. Hill, "The heat of shortening and the dynamic constants of muscle," *Proceedings of the Royal Society of London B: Biological Sciences, The Royal Society*, vol. 126, no. 843, pp. 136–195, 1938.

[4] A. Dwivedi, Y. Kwon, A. J. McDaid, and M. Liarokapis, "EMG based Decoding of Object Motion in Dexterous, In-Hand Manipulation Tasks," in *2018 7th IEEE International Conference on Biomedical Robotics and Biomechatronics (Biorob)*. IEEE, 2018, pp. 1025–1031.

[5] A. Dwivedi, L. Gerez, W. Hasan, C.-H. Yang, and M. Liarokapis, "A Soft Exoglove Equipped with a Wearable Muscle-Machine Interface based on Forcemyography and Electromyography," *IEEE Robotics and Automation Letters*, vol. 4, no. 4, pp. 3240–3246, 2019.

[6] O. Fukuda, T. Tsuji, M. Kaneko, and A. Otsuka, "A human-assisting manipulator teleoperated by emg signals and arm motions," *IEEE transactions on robotics and automation*, vol. 19, no. 2, pp. 210–222, 2003.

[7] Y. Kwon, A. Dwivedi, A. J. McDaid, and M. Liarokapis, "On Muscle Selection for EMG based Decoding of Dexterous, In-Hand Manipulation Motions," in *2018 40th Annual International Conference*

of the IEEE Engineering in Medicine and Biology Society (EMBC). IEEE, 2018, pp. 1672–1675.

[8] C. Loconsole, S. Dettori, A. Frisoli, C. A. Avizzano, and M. Bergamasco, "An EMG-based approach for on-line predicted torque control in robotic-assisted rehabilitation," in *2014 IEEE Haptics Symposium (HAPTICS)*. IEEE, 2014, pp. 181–186.

[9] N. Jiang, S. Dosen, K.-R. Muller, and D. Farina, "Myoelectric control of artificial limbs—is there a need to change focus?[in the spotlight]," *IEEE Signal Processing Magazine*, vol. 29, no. 5, pp. 152–150, 2012.

[10] N. Parajuli, N. Sreenivasan, P. Bifulco, M. Cesarelli, S. Savino, V. Niola, D. Esposito, T. J. Hamilton, G. R. Naik, U. Gunawardana *et al.*, "Real-time emg based pattern recognition control for hand prostheses: a review on existing methods, challenges and future implementation," *Sensors*, vol. 19, no. 20, p. 4596, 2019.

[11] A. Balbinot and G. Favieiro, "A neuro-fuzzy system for characterization of arm movements," *Sensors*, vol. 13, no. 2, pp. 2613–2630, 2013.

[12] K. Englehart and B. Hudgins, "A robust, real-time control scheme for multifunction myoelectric control," *IEEE transactions on biomedical engineering*, vol. 50, no. 7, pp. 848–854, 2003.

[13] D. Farina and R. Merletti, "Comparison of algorithms for estimation of EMG variables during voluntary isometric contractions," *Journal of Electromyography and Kinesiology*, vol. 10, no. 5, pp. 337–349, 2000.

[14] A. Phinyomark, F. Quaine, S. Charbonnier, C. Serviere, F. Tarpin-Bernard, and Y. Laurillau, "EMG feature evaluation for improving myoelectric pattern recognition robustness," *Expert Systems with applications*, vol. 40, no. 12, pp. 4832–4840, 2013.

[15] K. Englehart, B. Hudgin, and P. A. Parker, "A wavelet-based continuous classification scheme for multifunction myoelectric control," *IEEE Transactions on Biomedical Engineering*, vol. 48, no. 3, pp. 302–311, 2001.

[16] M. A. Oskoei and H. Hu, "Myoelectric control systems: A survey," *Biomedical Signal Processing and Control, Elsevier*, vol. 2, no. 4, pp. 275–294, 2007.

[17] A. Phinyomark, F. Quaine, S. Charbonnier, C. Serviere, F. Tarpin-Bernard, and Y. Laurillau, "EMG feature evaluation for improving myoelectric pattern recognition robustness," *Expert Systems with Applications, Elsevier*, vol. 40, no. 12, pp. 4832 – 4840, 2013.

[18] C. Kendell, E. D. Lemaire, Y. Losier, A. Wilson, A. Chan, and B. Hudgins, "A novel approach to surface electromyography: an exploratory study of electrode-pair selection based on signal characteristics," *Journal of Neuro Engineering and Rehabilitation, Elsevier*, vol. 9, no. 1, p. 24, 4 2012.

[19] B. Hudgins, P. Parker, and R. N. Scott, "A new strategy for multifunction myoelectric control," *IEEE Transactions on Biomedical Engineering, IEEE*, vol. 40, no. 1, pp. 82–94, 1993.

[20] K. Anam, R. N. Khushaba, and A. Al-Jumaily, "Two-channel surface electromyography for individual and combined finger movements," in *35th Annual International Conference of the IEEE Engineering in Medicine and Biology Society*, 2013, pp. 4961–4964.

[21] A. Dwivedi, G. Gorjup, Y. Kwon, and M. Liarokapis, "Combining Electromyography and Fiducial Marker based Tracking for Intuitive Telemanipulation with a Robot Arm Hand System," in *2019 28th IEEE International Conference on Robot and Human Interactive Communication (RO-MAN)*. IEEE, 2019, pp. 1–6.

[22] Y. Paul, V. Goyal, and R. A. Jaswal, "Comparative analysis between SVM & KNN classifier for EMG signal classification on elementary time domain features," in *4th IEEE International Conference on Signal Processing, Computing and Control, ISPCC 2017*. IEEE, 9 2017, pp. 169–175.

[23] R. N. Khushaba, A. Al-Timemy, S. Kodagoda, and K. Nazarpour, "Combined influence of forearm orientation and muscular contraction on EMG pattern recognition," *Expert Systems with Applications*, vol. 61, pp. 154–161, 2016.

[24] Y. Gu, D. Yang, Q. Huang, W. Yang, and H. Liu, "Robust EMG pattern recognition in the presence of confounding factors: features, classifiers and adaptive learning," *Expert Systems with Applications*, vol. 96, pp. 208–217, 4 2018.

[25] W. Geng, Y. Du, W. Jin, W. Wei, Y. Hu, and J. Li, "Gesture recognition by instantaneous surface EMG images," *Scientific Reports*, vol. 6, no. 1, p. 36571, 12 2016.

[26] G. Gao, A. Dwivedi, N. Elangovan, Y. Cao, L. Young, and M. Liarokapis, "The New Dexterity adaptive, humanlike robot hand," *IEEE International Conference on Robotics and Automation*, 2019.

[27] M. Quigley, K. Conley, B. P. Gerkey, J. Faust, T. Foote, J. Leibs, R. Wheeler, and A. Y. Ng, "ROS: an open-source Robot Operating System," in *ICRA Workshop on Open Source Software*, 2009.

[28] M. Asghari and O. HuoshengHu1, "Myoelectric control systems—a survey," *Biomedical Signal Processing and Control*, vol. 2, pp. 275–294, 2007.

[29] S. Zhang and B. Zhang, "The estimation of grasping force based on the feature extracted from emg signals," in *2016 IEEE Advanced Information Management, Communicates, Electronic and Automation Control Conference (IMCEC)*, Xi'an, China, 2006, pp. 1477–1480.

[30] A. Dwivedi, Y. Kwon, A. J. McDaid, and M. Liarokapis, "A Learning Scheme for EMG based Decoding of Dexterous, In-Hand Manipulation Motions," *IEEE Transactions on Neural Systems and Rehabilitation Engineering*, vol. 27, no. 10, pp. 2205–2215, 2019.

[31] A. Phinyomark, C. Limsakul, and P. Phukpattaranont, "Emg feature extraction for tolerance of white gaussian noise," 2008.

[32] H. H. Dennis Tkach and T. A. Kuiken, "Study of stability of time-domain features for electromyographic pattern recognition," *Journal of NeuroEngineering and Rehabilitation*, p. 21, 2010.

[33] A. Phinyomark, C. Limsakul, and P. Phukpattaranont, "A novel feature extraction for robust emg pattern recognition," *arXiv preprint arXiv:0912.3973*, 2009.

[34] E. Gokgoz and A. Subasi, "Comparison of decision tree algorithms for emg signal classification using dwt," *Biomedical Signal Processing and Control*, vol. 18, pp. 138–144, 2015.

[35] L. Breiman, "Random forests," *Machine learning, Springer*, vol. 45, no. 1, pp. 5–32, 2001.

[36] M. V. Liarokapis, P. K. Artemiadis, P. T. Katsiaris, K. J. Kyriakopoulos, and E. S. Manolakos, "Learning human reach-to-grasp strategies: Towards emg-based control of robotic arm-hand systems," in *2012 IEEE International Conference on Robotics and Automation*. IEEE, 2012, pp. 2287–2292.